Transaction B: Mechanical Engineering
Vol. 17, No. 2, pp. 93–101

SCIENTIA IRANICA

Comparing Sloshing Phenomena in a Rectangular Container with and without a Porous Medium Using Explicit Nonlinear 2-D BEM-FDM

M. Abbaspour[1,*] **and M. Ghodsi Hassanabad**[1]

Abstract. *The sloshing phenomena in a partially filled tank can affect its stability. Modifications of tank instability due to the movement of the tank carrier, are key design points for the stability of a carrier. Even though the sloshing phenomenon has already been investigated using the BEM-FDM technique, the research in this paper covers this phenomenon in a porous media, which is new in 2-D coordinates. For this purpose, a Laplace equation has been used for potential flow, and kinematic and dynamic boundary conditions have been applied to the free surface. Also, a formulation has been developed for a free surface in porous media. BEM has been used for solving the governing equation and FDM discretization has been used for kinematic and dynamic free surface boundary conditions and for time marching. Theoretical results have been verified with experimental data collected in this study. The results show an acceptable agreement between theory and experiment, and the rapid damping property in the sloshing phenomena by using porous material in the water, as expected. Also, these results illustrate that the derived formula in this research are applicable and true.*

Keywords: *Boundary Element Method (BEM); Finite Difference Method (FDM); Porous media; Potential flow; Liquid free surface.*

INTRODUCTION

Fluid flow models involving a deforming domain, in general, and free-surface flow models such as sloshing, in particular, have a similar challenge in their numerical simulation. These kinds of problem, especially with an interface-tracking approach, need moving mesh or regeneration of the domain mesh at each time step. Some difficulties, such as mesh regeneration and using more complex meshes, increase the solution time. The best approach for decreasing solution time is to use the BEM method to solve free-surface flows especially in potential flows.

Sloshing is one of the free-surface flows investigated for many applications. In the storage tanks of LNG tankers, sloshing produced by sea waves can affect the stability of the ship. The same phenomenon may happen when a trailer carrying any type of liquid passes over a road curve or a ramp. Hence, investigating the sloshing phenomena in these situations is a design key point for ensuring safety.

Many researchers have investigated sloshing phenomena by different theoretical and experimental methods. Faraday [1] began the first investigation of fluid sloshing in 1831. Then, in 1883, Rylie [1] assessed sloshing phenomena on a vibrating bed. In the 20th century, many researchers studied sloshing phenomena in horizontal, vertical and rotational motion (such as sway, heave and roll), 2-D and 3-D motion, and many other problems. In recent years, a wide range of articles have focused on sloshing, some of which have investigated the stability of containers due to sloshing. Liquid sloshing in ship tanks has been analyzed by Cariou and Casella [2]. Nasar et al. [3] set up an experimental study on liquid sloshing dynamics in a tank carrying barge. Wu [4] has investigated the resonance of sloshing in a tank. Liu and Lin [5] solved, numerically, liquid sloshing in tanks in three dimensions. The finite element method has been applied to solve the sway

1. *School of Mechanical Engineering, Sharif University of Technology, Tehran, P.O. Box 11155-9567, Iran.*
*. *Corresponding author. E-mail: m-abbaspour@jamejam.net*

Received 5 April 2009; received in revised form 25 July 2009; accepted 11 October 2009

linear and nonlinear motion of a 2-D container by Virilla et al. [6]. Hamano et al. [7] have used the boundary element method to model large amplitude standing waves in 2-D vessels. The boundary element method and the finite difference method have been used to model water wave motion with laminar boundary layers in a rectangular container by Jamali [8].

In recent years, a simple porous material (named Exess [9]) has been introduced as an anti-explosion product in storage tanks. In addition, these materials can improve the stability behavior of their carriers. The advantage of this material is that they only occupy 1.4 to 1.7 percent of the container space.

In this study, a new approach has been presented to solve free surface potential flow under non-linear boundary conditions in a rectangular container, with and without porous material. Moreover, a BEM-FDM model has been developed for sloshing in porous media.

METHODS

Mathematical Formulation

There is a wide range of motion that leads to sloshing phenomena. As a practical and important case, the maneuvering of a liquid tank carrier followed by a straight movement has been investigated. As a result of free surface experiences, the sloshing starts in a parabolic shape as shown in Figure 1.

Based on static relations in fluid mechanics, the initial condition of a fluid free surface would have a parabolic shape, which can be expressed as:

$$z = \frac{\omega^2}{2g}(R+x)^2 - \frac{R^2\omega^2}{2g},$$
$$\omega = \frac{U}{R}, \tag{1}$$

in which R, U and g are radius of curvature, carrier velocity and gravitational acceleration, respectively; x and z are horizontal and vertical coordinates (Figure 1).

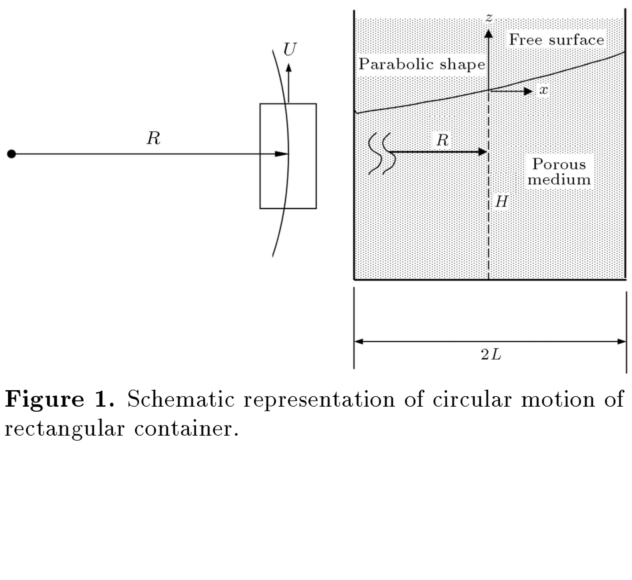

Figure 1. Schematic representation of circular motion of rectangular container.

Following the two dimensional free surface sloshing non-linear theory, the governing equation and boundary conditions are expressed as below [10].

By assuming irrotational flow, the governing equation is a Laplace equation in the form of:

$$\nabla^2\Phi = 0, \tag{2}$$

in which Φ is the potential function.

The kinematics boundary condition on the free surface is:

$$\frac{\partial\xi}{\partial t} = \frac{\partial\Phi}{\partial z} - \frac{\partial\Phi}{\partial x}\frac{\partial\xi}{\partial x}, \tag{3}$$

in which ξ is wave amplitude.

This relation is converted to [11]:

$$\frac{\partial\xi}{\partial t} = \frac{1}{\cos\beta}\frac{\partial\Phi}{\partial n}, \tag{4}$$

in which n is normal to the free surface and β is the angle the free surface makes with the horizontal line.

Applying Bernoulli's equation on a free surface provides the dynamic free surface boundary condition:

$$\frac{\partial\Phi}{\partial t} = B(t) - g\xi - \frac{1}{2}(\Delta\Phi)^2. \tag{5}$$

Using Equations 4 and 5, the dynamic free surface boundary condition is converted to [11]:

$$\left(\frac{\partial\Phi}{\partial t}\right)_x = B - g\xi - \frac{1}{2}\left[\left(\frac{\partial\Phi}{\partial s}\right)^2 - \left(\frac{\partial\Phi}{\partial n}\right)^2 - 2\frac{\partial\Phi}{\partial s}\frac{\partial\Phi}{\partial n}\tan\beta\right], \tag{6}$$

in which s is measured along the free surface and $(\partial\Phi/\partial t)_x$ indicates the rate of Φ change at a constant horizontal position, but following the free surface vertically.

The boundary condition on solid walls is:

$$\frac{\partial\Phi}{\partial n} = 0. \tag{7}$$

It is worth noting that the mentioned formulas are suitable for a container with only one type of fluid. If a liquid container is filled by a porous material, such as Exess, the related equations will differ.

Assuming irrotational flow, the governing equation in the porous media is the same Laplace equation. Also, the same is true for the kinematic boundary condition of a free surface and walls, i.e. Equations 4 and 7.

The dynamic boundary condition on a free surface, however, differs from the above equations (Equations 5 and 6). Neild et al. have presented the extension of Darcy's law, according to the Wooding paper, that can be applied for dynamic boundary conditions. The extension of Darcy's law is [12]:

$$\left[\frac{\partial V}{\partial t}+(V.\nabla)V\right]=-\frac{\nabla P}{\rho_f}-\frac{\mu}{\rho_f k}\vec{v}-g, \tag{8}$$

in which P, V, $\vec{v}$, ρ_f, k, μ and g are pressure, intrinsic average velocity, velocity vector, fluid density, permeability, viscosity and gravitational acceleration, respectively.

When the Dupuit-Forchheimer relationship is used, the above equation becomes [12]:

$$\left[\lambda^{-1}\frac{\partial \vec{v}}{\partial t}+\lambda^{-2}(\vec{v}.\nabla)\vec{v}\right]=-\frac{\nabla P}{\rho_f}-\frac{\mu}{\rho_f k}\vec{v}-g, \tag{9}$$

in which λ is porosity. This equation was obtained by analogy with the Navier-Stokes equation.

The irrotational flow theory leads to the relationship [13]:

$$(\vec{v}.\nabla)\vec{v}=\frac{1}{2}\nabla(\vec{v}.\vec{v}), \tag{10}$$

where:

$$\vec{v}=\nabla\Phi, \tag{11}$$

in which Φ and $\vec{v}$ are potential function and velocity vector, respectively.

By substituting Relations 10 and 11 in 9, the equation is simplified to:

$$\nabla\left(\frac{1}{\lambda}\frac{\partial\Phi}{\partial t}+\frac{1}{2\lambda^2}(\nabla\Phi)^2+\frac{P}{\rho_f}+\frac{\mu}{k\rho_f}\Phi+gz\right)=0, \tag{12}$$

and hence:

$$\frac{1}{\lambda}\frac{\partial\Phi}{\partial t}+\frac{1}{2\lambda^2}(\nabla\Phi)^2+\frac{P}{\rho_f}+\frac{\mu}{k\rho_f}\Phi+gz=B(t). \tag{13}$$

The above equation is similar to Equation 5 in general form. Equation 5 is Bernoulli's equation which has been obtained by a specified method [13]. In this study, a similar method has been used for deriving Equation 13 in a porous medium, which can be used for free surface dynamic boundary conditions.

Using the same method for converting the dynamic free surface boundary condition to a form of Equation 6, the following equation is obtained:

$$\left(\frac{\partial\Phi}{\partial t}\right)_x=B-\lambda g\xi-\frac{\mu\lambda}{k\rho}\Phi-\left[\frac{1}{2\lambda}\left(\frac{\partial\Phi}{\partial s}\right)^2-\left(1-\frac{1}{2\lambda}\right)\left(\frac{\partial\Phi}{\partial n}\right)^2-\frac{\partial\Phi}{\partial s}\frac{\partial\Phi}{\partial n}\tan\beta\right]. \tag{14}$$

Therefore, all formulas are equal for ordinary sloshing and sloshing in porous media, except under free surface dynamic boundary conditions. In other words, only Equation 5 differs from Equation 13.

Boundary Element Method

In order to solve the Laplace equation with all boundary conditions, the Green function is used and the governing equation can be transformed to the boundary integral equation shown as [14]:

$$\frac{\alpha}{2\pi}\Phi(p)=-\int_\Gamma\left[\Psi(p,q)\frac{\partial\Phi(q)}{\partial n_q}-\Phi(q)\frac{\partial\Psi(p,q)}{\partial n_q}\right]ds_q, \tag{15}$$

where:

$$\Psi=\frac{1}{2\pi}\ln r, \tag{16}$$

in which p is the source point and Ψ is the fundamental solution in the boundary element method.

In the boundary element method, after establishing the integral equation, it should be converted to an algebraic system of equations for obtaining potential functions and their derivatives on the nodes of the boundary. The following equation is concluded from the integral Equation 15 [14]:

$$[H]_{n\times n}[\Phi]_{n\times 1}=[G]_{n\times n}[\Phi_n]_{n\times 1}, \tag{17}$$

in which H and G are coefficient matrices; Φ and Φ_n are potential functions of boundary nodes and their normal derivatives to the boundary, respectively; and n is node numbers on the boundary. There are $2n$ unknown values in the set of Equation 17. These unknown values should be decreased to n unknown values. There are some Neumann boundary conditions (Equation 7) on the boundary of fluid in a rectangular container, which determine the values of Φ_n on the walls. Also, there are Robin boundary conditions (Equations 6 and 14) on the boundary of fluid in a rectangular container, which determine the relations between Φ and Φ_n on the free surface. These Robin boundary conditions should be discretized for each element because the specification of each node should be placed in Equation 17. The finite difference discretizing method is used for this purpose.

Finite Difference Method

Dirichlet and Neumann quantities of boundaries were obtained by discretizing the integral equation in the boundary element method. Time marching and the shape of the free surface at each time step requires the discretizing and solving of the kinematic and dynamic boundary conditions of the free surface. The finite difference method was selected for discretizing the free surface boundary conditions. The shape of the free surface was modified by spline interpolation at each time step.

The kinematic boundary condition on a free surface (Equation 3) of a container, with and without porous media, is discretized as below [11]:

$$\xi^{i+1} = \xi^i + \Delta t \left[\frac{a}{\cos\beta^{i+1}} \left(\frac{\partial\Phi}{\partial n}\right)^{i+1} + \frac{1-a}{\cos\beta^i} \left(\frac{\partial\Phi}{\partial n}\right)^i \right], \quad (18)$$

in which a is between 0 and 1. As seen in Equation 18, both iterations i and $i+1$ are at the right hand side of the equation. If 0 is replaced in a, then the right hand side of Equation 18 is only included by variables in iteration i and the formulation will be explicit. In the same manner if $a = 1$, then the formulation will be implicit, and if $0 < a < 1$, then the formulation will be composed of explicit and implicit.

Equation 18 is used for determining the new position of the free surface nodes in time marching and for applying it into Equations 19 and 20.

The dynamic boundary condition on the free surface (Equation 6) of a container without porous media is discretized, as below [11]:

$$\begin{aligned}
&\Phi^{i+1} + \Delta t \left[\frac{\text{bag}}{\cos\beta^{i+1}} \Delta t \right. \\
&\quad \left. -c \left(\frac{\partial\Phi}{\partial s}\right)^{i+1} \tan\beta^{i+1} \right] \left(\frac{\partial\Phi}{\partial n}\right)^{i+1} = \Phi^i \\
&\quad - g\Delta t \xi^i - g\Delta t^2 \frac{b(1-a)}{\cos\beta^i} \left(\frac{\partial\Phi}{\partial n}\right)^i \\
&\quad - \frac{1-c}{2} \Delta t \left[\left(\frac{\partial\Phi}{\partial s}\right)^2 - \left(\frac{\partial\Phi}{\partial n}\right)^2 \right. \\
&\quad \left. -2 \left(\frac{\partial\Phi}{\partial s}\right) \left(\frac{\partial\Phi}{\partial n}\right) \tan\beta \right]^i \\
&\quad - \frac{c}{2} \Delta t \left[\left(\frac{\partial\Phi}{\partial s}\right)^2 - \left(\frac{\partial\Phi}{\partial n}\right)^2 \right]^{i+1}, \qquad (19)
\end{aligned}$$

in which b and c are between 0 and 1. For the same reasons mentioned above, if $a = b = 0$, then the formulation of Equation 19 will be explicit.

The dynamic boundary condition on the free surface (Equation 14) of a container with porous media is discretized after some lengthy and new operations, as below:

$$\begin{aligned}
&\left(1 + d\frac{\mu\lambda}{K\rho_f}\Delta t\right)\Phi^{i+1} + \Delta t \left[\frac{\lambda\text{bag}}{\cos\beta^{i+1}} \Delta t \right. \\
&\quad \left. -c \left(\frac{\partial\Phi}{\partial s}\right)^{i+1} \tan\beta^{i+1} \right] \left(\frac{\partial\Phi}{\partial n}\right)^{i+1} \\
&\quad = \left(1 - \frac{\mu\lambda(1-d)}{k\rho_f}\right)\Phi^i - g\Delta t \lambda \xi^i \\
&\quad - g\Delta t^2 \frac{\lambda b(1-a)}{\cos\beta^i} \left(\frac{\partial\Phi}{\partial n}\right)^i \\
&\quad - (1-c)\Delta t \left[\frac{1}{2\lambda} \left(\frac{\partial\Phi}{\partial s}\right)^2 - \left(1 - \frac{1}{2\lambda}\right) \left(\frac{\partial\Phi}{\partial n}\right)^2 \right. \\
&\quad \left. - \left(\frac{\partial\Phi}{\partial s}\right) \left(\frac{\partial\Phi}{\partial n}\right) \tan\beta \right]^i - c\Delta t \left[\frac{1}{2\lambda} \left(\frac{\partial\Phi}{\partial s}\right)^2 \right. \\
&\quad \left. - \left(1 - \frac{1}{2\lambda}\right) \left(\frac{\partial\Phi}{\partial n}\right)^2 \right]^{i+1}. \qquad (20)
\end{aligned}$$

Equations 19 and 20 follow the same conditions for implicit or explicit states.

Equations 19 and 20 are used for determining the potential function and its derivative of free surface nodes in time marching. Also, the derivative of the potential function relative to s (tangential line) is obtained by finite difference approximation in the previous time step (iteration i).

Some Numerical Considerations

Three constant parameters (a, b, c) were introduced in Equations 18 to 20. a, b and c are between zero and 1. If these three parameters are equal to 1, the solution will be fully implicit, because all terms in Equations 18 to 20 are in iteration $i+1$. However, if they are equal to zero, the solution will be fully explicit, because all terms in Equations 18 to 20 will be in iteration i.

Different quantities of these parameters determine the weight of different implicit and explicit terms in the equations.

In this study, the fully explicit formulations ($a = b = c = 0$) were chosen due to their easiness.

Also, Table 1 shows the other specifications of the sloshing model.

Pressure on the side walls for calculating non-dimensional forces can be obtained by Bernoulli's equation (Equation 5) for a container filled with liquid only and derived equation (Equation 13) for a container with porous material. In this study, the non-dimensional forces on the side walls have been computed in terms of non-dimensional time.

Table 1. The main parameters used in the numerical method.

Parameters	Quantity	Descriptions
U (m/s)	1	Carrier velocity
L (m)	0.2	$2L$ is the length of rectangular container
H (m)	0.2	The height of rectangular container
R (m)	1	Radius of curvature
Δt (sec)	0.01	Time step
No. F. elements	40	Number of free surface elements
No. T. elements	120	Number of total elements on the boundaries
λ	0.4	The porosity of domain which is near to the low dense wire crimps domain
K (m^2)	8×10^{-11}	The permeability of domain which is near to the low dense wire crimps domain

Experimental Method

In the present study, an experimental set up was applied for verifying the numerical data obtained in this study. As shown in Figure 2, a parabolic plane was used to shape the water free surface of the container as a parabola. This parabola matches the numerical dimensions of this research and Equation 1. Also, low dense wire crimps have been used as the porous material.

For initializing the experiment, the parabolic plane was put on the water free surface. Then, this plane was taken away quickly in order to observe the tank surface behavior. The sloshing phenomenon occurred due to gravity, surface tension etc. with gravity as the dominant factor. The edges of the parabolic plane were sealed to prevent water penetration. Also, in this simple setup, unwanted side effects such as sloshing due to intense air flow under the plane were prevented by making some holes on the upper part of the parabolic plane. The surface tension, however, is unavoidable. It is the main reason for differences between numerical and experimental results, but it can be detected from gravitational waves by observation.

RESULTS

Figures 3 and 4 show some real pictures of free surface motion, compared to numerical results. Cyan curves show the numerical data of this research. As shown in Figure 3a, in the 0.1 sec after the initial condition, the free surface of the water in the experiment coincides with the numerical sample. In Figure 3b, after 1 sec, the water surface reaches near its equilibrium surface. In this case, some waves are seen on the water surface, but the main line of the free surface coincides with theoretical results.

In Figure 3c, the free water surface passes from its equilibrium line, and hence the other end of the free surface goes up. As shown in this figure, ignoring the waves with small wave lengths, the free surface of the experimental data coincides properly with numerical results. Also, according to Figures 3d to 3k, the numerical motion of the free surface curve coincides acceptably with experimental wave shapes.

According to Figure 4a, in the case of using porous material in the container, the cyan curve extracted from the numerical results under initial conditions coincides with the free surface of the water. In

Figure 2. Image of experimental device.

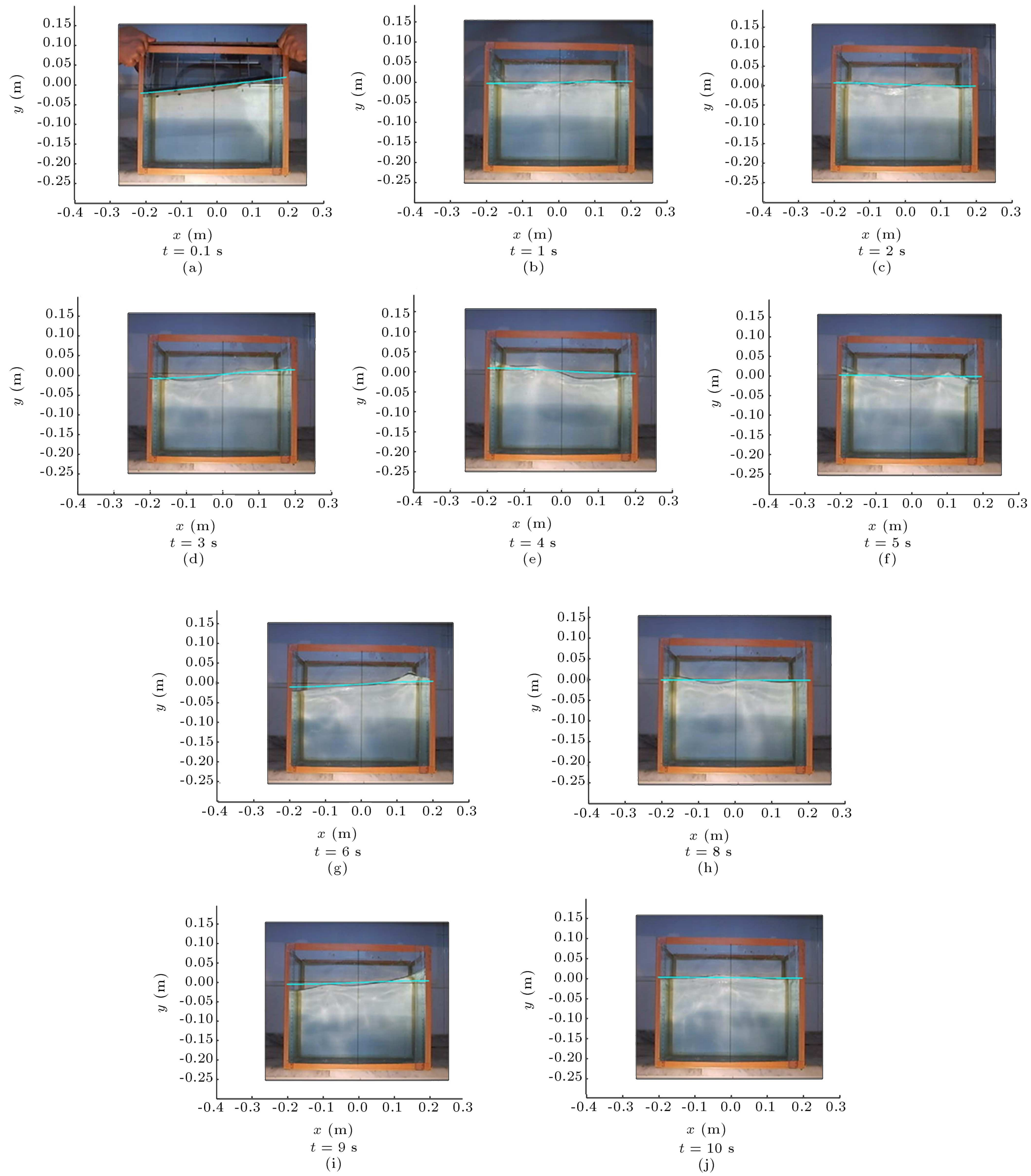

Figure 3. Images of water sloshing from 0.1 s to 10 s (comparing numerical and experimental data).

Figure 4b, after 0.2 sec, the computed curve moves with the same pattern of the experimental free surface motion. Also, in other parts of Figure 4, there is a good match between experimental and numerical results. As shown in Figure 4, the resulted wave is completely damped after a complete period, which is 1.08 sec.

Figure 5 shows the non-dimensional forces on the side walls, with respect to non-dimensional time, which is obtained by the numerical calculation of the present research. The rapid damping property of porous materials is illustrated in Figure 5 very well, as expected. In this figure, L is 20 cm, ρ is about

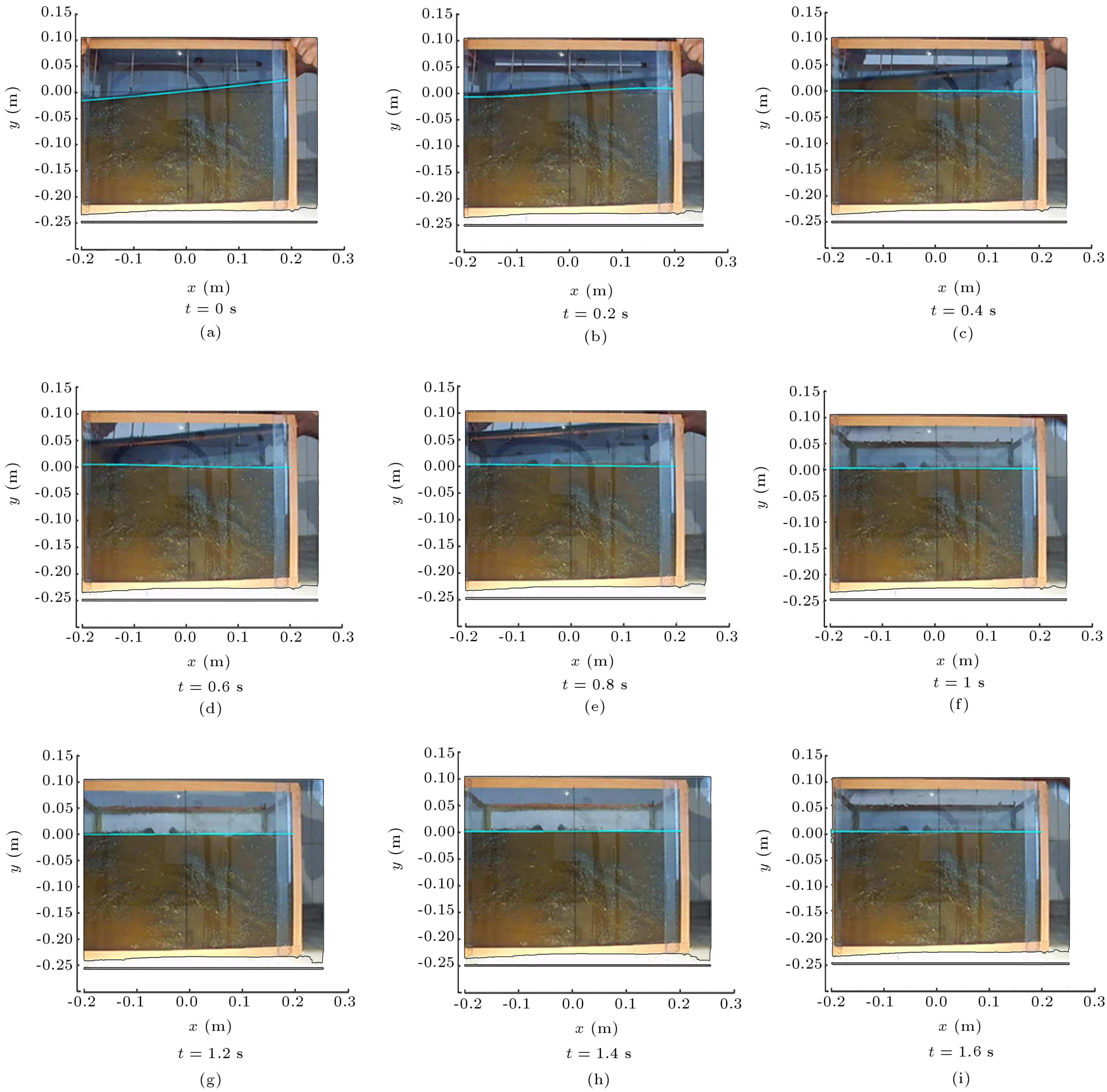

Figure 4. Images of water sloshing from 0 sec to 1.6 sec in porous media (comparing numerical and experimental data).

1000 kg/m^3, g is 9.81 m/s^2 and after around 1.4 sec the force is damped.

Figure 6 shows the right end of the free surface displacement, experimentally and numerically, in the container filled just by water. This figure shows an acceptable agreement between experiment and computation.

Figure 7 shows the right end of the free surface displacement, experimentally and numerically, in the container filled with porous material. This figure shows a very good coincidence between experiment and computation. In this figure, the amplitude damps in around 1.35 sec.

DISCUSSION AND CONCLUSION

Kukner and Baykal have investigated sloshing phenomena due to triangular initial free surface. They showed that utilizing triangular corrugated bottoms may help to regulate the flow in tanks [15].

Corrugated bottoms were not used in the present research; instead, porous material was placed in the container in order to increase the stability of the tank. In addition, a parabolic shape was used for the initial free surface. The research of Kukner and Baykal [15], as well as the present research, tries to introduce a method to augment the stability of tanks. It seems

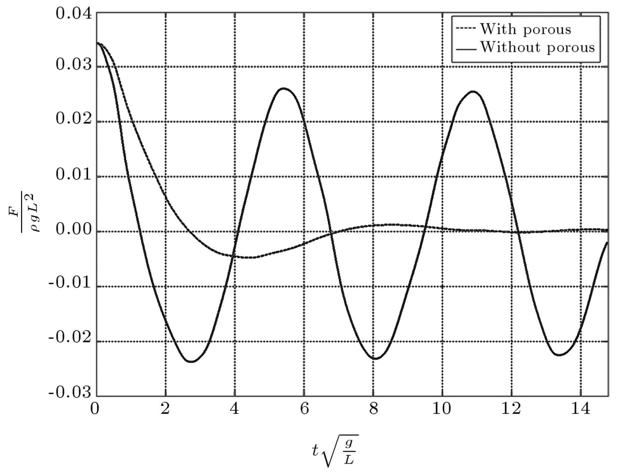

Figure 5. Comparison of non-dimensional wall forces in terms of non-dimensional time in a rectangular container with porous material and only filled by water.

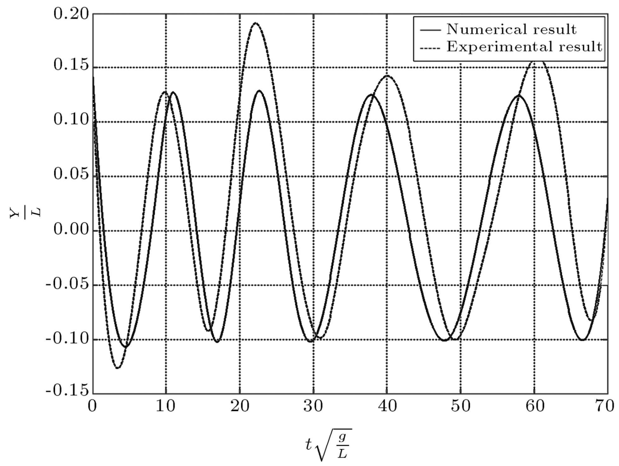

Figure 6. Free surface right end displacement for comparing numerical and experimental results in a container filled just with water.

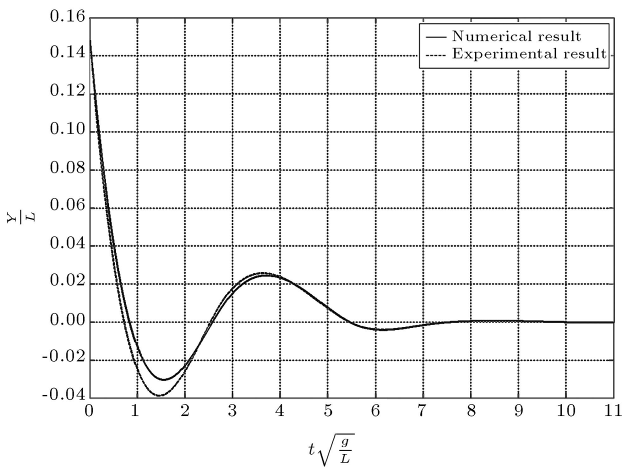

Figure 7. Free surface right end displacement for comparing numerical and experimental results in the container with porous material.

that the method of the present study is more useful, because of the more rapid damping of sloshing forces.

One of the most important problems in ship LNG tanks is sloshing. Graczyk and Moan studied this subject and showed that the level of free surface affects the sloshing forces on the tank walls [16]. In this research, a parabolic shape was used for the initial free surface, which can be similar to the result of ship maneuvering. According to the results of this research, it is proposed that, to decrease this sloshing effect, it is proper to use porous materials.

In the present research, some differences were observed between experimental and numerical results. The experiment indicated that when the parabolic plane is taken away, gravity and surface tension create two types of wave. The first wave is due to gravity, with a wave length of $4L$ (container length is $2L$); in this case, the amplitude of free surface motion in the middle of the container is about zero. The second wave is due to surface tension; with a wave length of about L (container length is $2L$). Ignoring the effects of the second wave leads to an acceptable similarity between the theoretical and experimental results.

In conclusion, using porous media is an excellent idea for rapid damping of the sloshing phenomenon. Experimental results indicated that the wave damps in about one second in a porous container, while taking about twenty seconds without a porous medium. A similar trend occurs for wave forces exerted on the container walls.

REFERENCES

1. Ibrahim, A., *Liquid Sloshing Dynamics: Theory and Applications*, Cambridge University Press, pp. 20-40 (2005).
2. Cariou, A. and Casella, G. "Liquid sloshing in ship tanks: a comparative study of numerical simulation", *Marine Structures*, **12**, pp. 183-198 (1999).
3. Nasar, T. et al. "Experimental study of liquid sloshing dynamics in a barge carrying a tank", *Fluid Dynamics Research*, **40**, pp. 427-458 (2008).
4. Wu, G.X. "Second-order resonance of sloshing in a tank", *Ocean Engineering*, **34**, pp. 2345-2349 (2007).
5. Liu, D. and Lin, P. "A numerical study of three-dimensional liquid sloshing in tanks", *Journal of Computational Physics*, **227**, pp. 3921-3939 (2008).
6. Virilla, J.C. et al. "Linear and nonlinear 2-D finite element analysis of sloshing modes and pressures in rectangular tanks subject to horizontal harmonic motions", *Journal of Sound and Vibration*, **312**, pp. 442-460 (2008).
7. Hamano, K. et al. "Boundary element simulation of large amplitude standing waves in vessels", *Engineering Analysis with Boundary Elements*, **27**, pp. 565-574 (2003).

8. Jamali, M. "BEM modeling of surface water wave motion with laminar boundary layers", *Engineering Analysis with Boundary Elements*, **30**, pp. 14-21 (2006).
9. "Anti explosion systems", http://exesslibya.com/4main.htm.
10. Dean, R.G. and Dalrymple, R.A., *Water Wave Mechanics for Engineers and Scientists*, 3rd Edition, World Scientific, pp. 35-66 (1991).
11. Liu, P.L. and Liggett, J.A. "Application of boundary element methods to problems of water waves", in *Developments in Boundary Element Methods-2*, P.K. Banerjee and R.P. Shaw, Eds., Applied Science Publishers LTD, pp. 37-67 (1982).
12. Nield, D.A. and Bejan, A., *Convection in Porous Media*, 3rd Edition, Springer, Science+Business Media Inc, pp. 8-15 (2006).
13. White, F.M., *Fluid Mechanics*, 6th Ed., McGraw-Hill Science Engineering (2006).
14. Katsekadelis, J.T., *Boundary Elements: Theory and Applications*, First Ed., Elsevier Science Pub. Co. (2002).
15. Kukner, A. and Baykal, M.A. "Wave sloshing in corrugated bottom tanks with two-dimensional flow", *Ocean Engineering*, **26**, pp. 703-712 (1999).
16. Graczyk, M. and Moan, T. "A probabilistic assessment of design sloshing pressure time histories in LNG tanks", *Ocean Engineering*, **35**, pp. 834-855 (2008).

BIOGRAPHIES

Madjid Abbaspour received his BS degree in mechanical engineering from Sharif University of Technology (SUT) in 1973, his MS in thermal energy from the Massachussets Institute of Technology (MIT) in 1975, and his PhD degree in civil and environmental engineering from Cornell University in 1980, with a minor in ocean engineering. Since then he has served in SUT as a faculty member. He has published more than 13 books in his related field and more than 150 papers in respected journals and international conference proceedings. In 1995, he was honored to receive an award for the best published book in the field of engineering, entitled "Environmental Engineering". Prof. Abbaspour is the chief editor of the ISI ranked "International Journal of Environmental Science and Technology" (IJEST). He has won many academic awards and also the national medal of merit for outstanding research activities (1997). He has two registered inventions in the field of ocean and marine engineering (2009). He also won the 10th and 12th Kharazmi international awards, respectively, in 1997 and 1999, in the field of research and innovation.

Madjid Ghodsi Hasanabad received a BS in mechanical engineering (solid mechanics) from Tehran University in 2000 and a MS in mechanical engineering (fluid mechanics) from Sharif University of Technology, Tehran, in 2003. He has been working since 2004 on his doctoral project in 'free surface flows', and 'boundary element method' at Sharif University of Technology. He has published more than 15 papers in journals and conference proceedings. He has one registered invention in the field of refrigeration (2008) and in 2001 he won the Iranian mechanical engineers society award for the best BS thesis in solid mechanics.